PERFORMANCE ANALYSIS AND RANGE IMPROVEMENT IN MULTIBAND-OFDM UWB COMMUNICATIONS

Qiyue Zou, Alireza Tarighat, and Ali H. Sayed

Electrical Engineering Department
University of California
Los Angeles, CA 90095
Email: {eqyzou,tarighat,sayed}@ee.ucla.edu

ABSTRACT

The performance of multiband-OFDM UWB systems is analyzed using the S-V indoor channel model. Based on the analysis, two methods are proposed to improve the reliable transmission range of UWB devices by exploiting the rich spectral and spatial diversity available in the system. It is shown both by theory and computer simulations that the proposed methods can effectively enlarge the transmission range of UWB devices.

1. INTRODUCTION

Ultra-wideband (UWB) communication technology is emerging as a leading standard for high data rate applications over wireless networks [1]. Due to its use of a high frequency bandwidth, UWB allows the wireless connection of multiple devices at very high data rates. The interest in UWB systems has been sparked by an order issued by the Federal Communications Commission (FCC) in February 2002 [2]. In this order, the FCC allocated a range of bandwidth from 3.1 GHz to 10.6 GHz for unlicensed use by UWB transmitters at a limited transmission power of -41.25 dBm/MHz or less.

An OFDM-based physical layer is one of the promising options for UWB devices due to its capability to capture multipath energy and eliminate inter-symbol interference and the fact that OFDM is considered by the industry as a mature and reliable technology [3]. For these reasons, our focus will be on the OFDM-based modulation scheme for UWB communications. Despite the merits mentioned above, the extremely short range, e.g., 10 meters for a data rate of 110 Mbps, puts UWB at an obvious disadvantage when compared to other competitive technologies, such as the soon coming IEEE 802.11n standard, which supports a data rate of 200 Mbps for at least 40 meters in indoor environments. Hence, in order to push UWB as an attractive option for Wireless Personal Area Network (WPAN) applications, it is crucial to improve the range limit of UWB devices.

In the sequel, we first give a brief introduction of the multiband-OFDM modulation scheme that is proposed by the IEEE 802.15.3a standardization group for UWB communications [3]. Then we present analytical results on the coded BER and link PER versus distance in the multiband-UWB system using a practical channel model [4]. The derivations allow us to examine the achievable transmission range analytically. Furthermore, two methods are presented to improve the reliable transmission range of UWB devices by exploiting coding techniques at the transmitter as well as multiple antenna configurations.

This material was based on work supported in part by the National Science Foundation under award ECS-0401188.

2. MULTIBAND-OFDM UWB SYSTEMS

In a multiband-OFDM UWB system, the spectrum is divided into several sub-bands of bandwidth 528 MHz each. The system operates in one sub-band and then switches to another sub-band after a short time. The transmitted symbols are time interleaved across the sub-bands to utilize the spectral diversity to improve the reliability of transmission. In each sub-band, OFDM modulation is used to transmit data symbols [5]. The fundamental transmitter and receiver structure of a multiband-OFDM system is illustrated in Figs. 1 and 2. At the transmitter, the bits from information sources are first whitened by the scrambler and then encoded by the convolutional encoder. In order to exploit time-frequency diversity and combat multipath fading, the coded bits are further interleaved according to some preferred time-frequency pattern, and the resulting bit sequence is mapped into constellation symbols and then converted into a block of N symbols $x[0], \ldots, x[N-1]$ by the serial-to-parallel converter. The N symbols are the frequency components to be transmitted using the N subcarriers of the OFDM modulator, and are converted to OFDM symbols $X[0], \ldots, X[N-1]$ by the unitary inverse Fast Fourier Transform (IFFT). After adding a cyclic prefix of length P, the resulting $N+P$ time-domain symbols are converted into a continuous-time signal $x(t)$ for transmission.

At the receiver, the received block after OFDM demodulation is given by $y[0]$, ..., $y[N-1]$, whose elements are related to the frequency response of the channel by

$$y[k] = H[k]x[k] + w[k], \quad k = 0, \ldots, N-1. \qquad (1)$$

Here, $x[k]$ is the transmitted symbol in the k^{th} subcarrier, $H[k]$ is the channel response in the k^{th} subcarrier, and $w[k]$ is the additive noise component in the k^{th} subcarrier. Note

that $H[k]$, $k = 0, \ldots, N-1$, are the Fourier transform coefficients of the discrete-time baseband channel impulse response. From (1), $x[k]$ can be simply estimated from $\widehat{x}[k] = y[k]/H[k]$. The obtained symbols are then mapped into bits, and the resulting bit sequence is deinterleaved and decoded to get back the information bits.

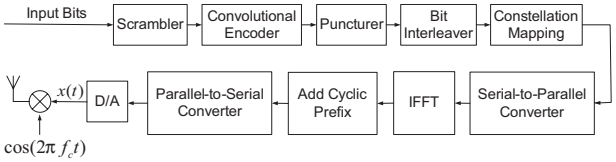

Fig. 1. Block diagram of the transmitter of a multiband-OFDM system.

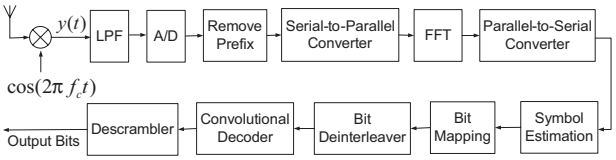

Fig. 2. Block diagram of the receiver of a multiband-OFDM system.

3. PERFORMANCE ANALYSIS

In order to examine the system performance, we shall use the S-V channel model that has been proposed by the IEEE 802.15.3a working group in order to evaluate different UWB communication schemes [4].

3.1. S-V Model

In this model, the impulse response of the multipath channel is modeled as

$$h(t) = X \sum_{l=0}^{L} \sum_{m=0}^{M} \alpha_{m,l} \delta(t - T_l - \tau_{m,l}),$$

where $\alpha_{m,l}$ is the multipath gain coefficient, T_l is the delay of the l^{th} cluster, $\tau_{m,l}$ is the delay of the m^{th} multipath component relative to the l^{th} cluster arrival time, and X represents Log-normal shadowing. The distribution of the cluster arrival time and the ray arrival time is

$$p(T_l|T_{l-1}) = \Lambda e^{-\Lambda(T_l - T_{l-1})},$$
$$p(\tau_{m,l}|\tau_{m-1,l}) = \lambda e^{-\lambda(\tau_{m,l} - \tau_{m-1,l})},$$

where Λ and λ are the cluster arrival rate and the ray arrival rate, respectively. The profile of the power decay along different propagation paths is described by

$$\mathbf{E}\{|\alpha_{m,l}|^2\} = \Omega_0 e^{-\frac{T_l}{\Gamma}} e^{-\frac{\tau_{m,l}}{\gamma}},$$

where Γ and γ are constants that characterize the exponential decay of each cluster and each ray in its associated cluster. The large-scale fading coefficient X is modeled as a Log-normal random variable, i.e., $20\log_{10} X \propto \mathcal{N}(0,\ \sigma_x^2)$, while the total energy contained in the terms $\alpha_{m,l}$ is normalized to unity for each channel realization.

The constant parameters in this model can be specified to account for different indoor environments. The IEEE 802.15.3a working group defined four types of indoor channels, namely CM1, CM2, CM3, and CM4 models. In the paper, our simulations are based on the CM3-type channel model.

3.2. Statistical Characteristics of $H[k]$

It can be derived from the channel model that $\mathbf{E}\{H[k]\} = 0$ and $\mathbf{E}\{|H[k]|^2\} = e^{0.0265\sigma_x^2}$. When L and M are large, it is reasonable to assume that $H[k]$ is circularly symmetric and Gaussian distributed by the central limit theorem. Hence, the probability density function of $|H[k]|^2$ can be approximated by the exponential distribution:

$$p(|H[k]|^2) \approx \frac{1}{\mathbf{E}\left\{|H[k]|^2\right\}} e^{-\frac{|H[k]|^2}{\mathbf{E}\{|H[k]|^2\}}}.$$

Moreover, the normalized cross-correlation of $H[k]$ is given by

$$\left| \frac{\mathbf{E}\{H[k_1]H^*[k_2]\}}{\mathbf{E}\left\{|H[k]|^2\right\}} \right| \approx \left| \frac{1 + \frac{\Lambda\Gamma}{1 + j\frac{2\pi(\overline{k}_1 - \overline{k}_2)\Gamma}{NT_s}}}{1 + \Lambda\Gamma} \right| \cdot \left| \frac{1 + \frac{\lambda\gamma}{1 + j\frac{2\pi(\overline{k}_1 - \overline{k}_2)\gamma}{NT_s}}}{1 + \lambda\gamma} \right|$$

where T_s is the symbol time and $\overline{k}_i$ is related to k_i by

$$\overline{k}_i = \begin{cases} k_i, & 0 \le k_i \le \frac{N}{2} - 1, \\ k_i - N, & \frac{N}{2} \le k_i \le N - 1. \end{cases}$$

for $i = 1, 2$. Two subcarriers k_1 and k_2 can be regarded as uncorrelated if their normalized cross-correlation is small. For example, it can be estimated from the above equation with a threshold 0.5 that the coherent bandwidth of the CM3-type channels is about 20.6 MHz.

3.3. Average BER and PER

Using the distribution of $|H[k]|^2$, we can now evaluate the average bit error rate (BER) and packet error rate (PER) of the multiband-OFDM UWB scheme. In the following analysis, we assume a QPSK constellation.

1.) Average uncoded BER (BER before the convolutional decoder):

$$\mathrm{BER}_{\mathrm{uc}} = \frac{1}{2}\left(1 - \sqrt{\frac{\mathrm{SNR}_{\mathrm{r}}}{1 + \mathrm{SNR}_{\mathrm{r}}}}\right),$$

where $\mathrm{SNR}_{\mathrm{r}} = \frac{E_b}{N_0}$ is the signal-to-noise ratio at the receiver, E_b is the average received energy per bit, and N_0 is the single-sided power spectral density of the additive white Gaussian noise.

2.) Average coded BER (BER after the convolutional decoder): Assume that the convolutional encoder is followed by an *ideal* time-frequency interleaver. Then,

$$\mathrm{BER}_{\mathrm{c}} \le \left.\frac{\partial T(W, I)}{\partial I}\right|_{I=1, W=\sqrt{4\mathrm{BER}_{\mathrm{uc}}(1-\mathrm{BER}_{\mathrm{uc}})}}, \qquad (2)$$

where $T(W, I)$ is the generating function of the convolutional encoder. Expression (2) can be approximated by

$$\mathrm{BER_c} \approx N_b \left[4\,\mathrm{BER_{uc}}\,(1-\mathrm{BER_{uc}})\right]^{\frac{d_{free}}{2}}, \qquad (3)$$

where d_{free} is the minimum free distance of the convolutional code, and N_b is the sum of the Hamming weight of all the input sequences whose associated convolutional codewords have a Hamming weight of d_{free} [6]. For the convolutional encoder specified in the multiband-OFDM proposal, $d_{free} = 15$ and $N_b = 7$.

3.) Average PER: Assume each packet consists of U information bits, and each information bit has the same probability of being decoded wrongly. Thus,

$$\mathrm{PER} = 1 - (1 - \mathrm{BER_c})^U. \qquad (4)$$

4.) UWB Link Budget: Since the transmission power must not exceed the specified -41.25 dBm/MHz, the average transmitted power should satisfy

$$P_{TX} \leq -41.25 + 10\log_{10}(f_U - f_L)\ (\mathrm{dBm}), \qquad (5)$$

where f_U and f_L are the upper and lower frequencies in terms of MHz of the transmission spectrum. The signal attenuation during transmission is modeled by the path loss $P_L = 20\log_{10}(4\pi f_g d/c)$ (dB), where c is the speed of light, f_g is the geometric average of f_U and f_L, and d is the transmission distance [5]. At the receiver, the average noise power per bit can be computed using the formula $-174 + 10\log_{10}R_b$ (dBm), where R_b is the data rate in bps and -174 is due to the thermal noise generated at the receive antenna. Thus, the received $\mathrm{SNR_r} = \frac{E_b}{N_0}$ is related to d by

$$\mathrm{SNR_r} = P_{TX} - 20\log_{10}\left(\frac{4\pi f_g d}{c}\right) - (-174 + 10\log_{10}(R_b)) - 6.6 - 2.5 + 10\log_{10}\left(\mathbf{E}\left\{|H[k]|^2\right\}\right)\ (\mathrm{dB}),$$

where 6.6 (dB) is the noise figure of antenna and receiver RF chain, and 2.5 (dB) is the implementation loss.

3.4. 90^{th}-Percentile BER and PER

In addition to the average BER and PER performance, we are also interested in another form of performance measure that gives an indication of the probability of channel failure. For this purpose, the so-called "90^{th}-percentile BER (or PER) performance" [5] is defined as the BER (or PER) level such that the multiband-OFDM scheme will perform better than at least 90% of the channel realizations. Since it is cumbersome to compute the 90^{th}-percentile performance measure explicitly, we shall approximate it as follows. We first identify the cutoff channel gain such that 90% of the subcarrier channel realizations will exceed it. This is found by setting

$$F(|H_{90\%}[k]|^2) \approx 1 - e^{-\frac{|H_{90\%}[k]|^2}{\mathbf{E}\{|H[k]|^2\}}} = 0.10,$$

i.e., the cutoff gain is

$$|H_{90\%}[k]|^2 = -\ln(0.9)\,\mathbf{E}\{|H[k]|^2\} = 0.105\,\mathbf{E}\{|H[k]|^2\}.$$

Then, we use this gain to approximate the 90^{th}-percentile uncoded BER as

$$\mathrm{BER_{uc,90\%}} \approx Q\left(\sqrt{0.210\,\mathrm{SNR_r}}\right).$$

The corresponding 90^{th}-percentile coded BER and PER can be calculated explicitly using (3) and (4) with $\mathrm{BER_{uc}}$ replaced by $\mathrm{BER_{uc,90\%}}$.

4. RANGE IMPROVEMENT

We now show how to exploit linear precoding and multiple antennas in multiband-OFDM systems to improve the reliable transmission range of UWB communications. The linear precoding approach trades range with decoding complexity, while the multiple antenna approach requires extra hardware and RF links.

4.1. Precoding over Parallel OFDM Subcarriers

It is seen from (3) that the use of a convolutional code with a bit interleaver for OFDM modulation can achieve a coding gain that is represented by the exponent of the $\mathrm{SNR_r}$ term, i.e., $\frac{d_{free}}{2}$. However, in UWB systems, there exists rich spectral and spatial diversity that may exceed what can be achieved by a convolutional code of moderate complexity. For example, the coherence bandwidth of the CM3-type channels is about 20.6 MHz, which is much smaller than the bandwidth of each sub-band, i.e., 528 MHz. Moreover, from expression (3), we notice that a small improvement in the uncoded BER will benefit the overall system performance, such as the PER, significantly through the exponential effect. This observation motivates us to use linear precoding to improve the uncoded BER [7].

Assume that we intend to send S symbols using J independent subcarriers ($J \geq S$). Instead of transmitting the original constellation symbols, we send rotated symbols that are obtained by

$$\left[\ x'[k_1] \quad \ldots \quad x'[k_J]\ \right]^T = \mathbf{A} \cdot \left[\ x[k_1] \quad \ldots \quad x[k_S]\ \right]^T,$$

where $\mathbf{A}^*\mathbf{A} = \frac{J}{S} \cdot \mathbf{I}_S$, and $\mathbf{A}$ is selected to maximize the minimum product distance between any two rotated code vectors, i.e.,

$$\mathbf{A} = \arg\max_{\mathbf{A}} \min_{\mathbf{x}'_1 \neq \mathbf{x}'_2} \prod_{j=1}^{J} |x'_1[k_j] - x'_2[k_j]|,$$

where $\mathbf{x}'_i = \left[\ x'_i[k_1] \quad \ldots \quad x'_i[k_J]\ \right]^T$, $i = 1, 2$, are two rotated code vectors. To decode the original symbols, sphere decoding can be used as a sub-optimal approximation to the maximum likelihood decoding at a relatively lower complexity. For example, in order to implement the precoding scheme with $S = 2$, $J = 2$, we group the subcarriers in a sub-band according to the pairing $\left(k,\ k + \frac{N}{2}\right),\ k = 0, \ldots, \frac{N}{2} - 1$. The symbols $x[k]$ and $x[k + \frac{N}{2}]$ are converted to $x'[k]$ and $x'[k + \frac{N}{2}]$, which are transmitted over subcarriers k and $k + \frac{N}{2}$, respectively.

Original scheme	Precoding - S=2, J=2	Precoding - S=3, J=3	1T×2R×	2T×1R×	2T×2R×
11.8 m	15.8 m	18.8 m	25.4 m	18.1 m	34.0 m

Table 1. Table of achievable range for a 90^{th}-percentile PER 0.08 when $R_b = 110$ Mbps.

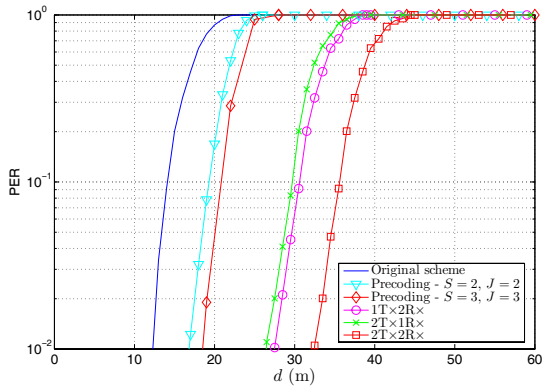

Fig. 3. Plot of simulated average PER vs. distance.

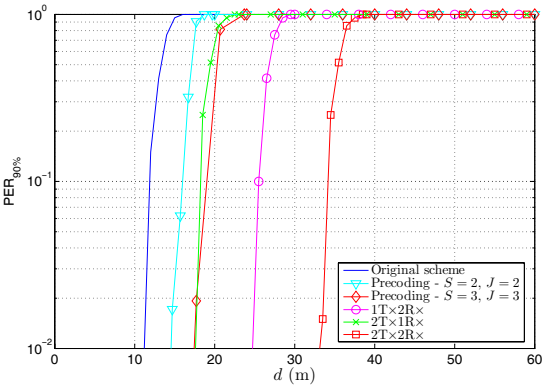

Fig. 4. Plot of simulated 90^{th}-percentile PER vs. distance.

4.2. MIMO Scheme

We can also exploit multiple transmit and receive antennas to improve the transmission range of UWB devices. For ease of decoding, the most commonly used schemes consist of the 1T×2R×, 2T×1R×, and 2T×2R× schemes. For example, the 1T×2R× scheme uses one transmit antenna and two receive antennas, and we can apply the maximal ratio combiner [8] to achieve the optimal performance given by

$$\mathrm{BER}_{\mathrm{uc}}^{1\mathrm{T}\times 2\mathrm{R}\times} = \frac{1}{2} - \frac{3}{4}\mu + \frac{1}{4}\mu^3,$$

where $\mu = \sqrt{\frac{\mathrm{SNR_r}}{1+\mathrm{SNR_r}}}$.

5. COMPUTER SIMULATIONS

In this section, we verify the expected range improvement using computer simulations. The multiband-OFDM UWB system proposed by the IEEE 802.15.3a working group is implemented using MATLAB. In the simulations, we utilize the bandwidth from 3.1 GHz to 4.8 GHz with the average transmission power $P_{TX} = -10.3$ dBm, which satisfies (5). The data rate is $R_b = 110$ Mbps, and the packet length is 1024 bytes. The OFDM symbol size is 128. For more details about the system, such as the convolutional encoder and the bit interleaver, we refer to [3]. In order to measure the PER performance, 200 channel realizations are generated, and for each channel realization 400 packets of random bits are sent and received using the system. In Figs. 3 and 4, the simulated average and 90^{th}-percentile PERs in the CM3-channel environment are plotted vs. the transmission distance for the different schemes discussed in this paper. Table 1 lists the maximal transmission range when the required 90^{th}-percentile PER is less than 0.08. The use of multiple antennas can improve the reliable transmission range more significantly compared to linear precoding; however, linear precoding does not require extra antennas and RF links.

6. CONCLUSIONS

In the paper, we studied the performance of multiband-OFDM UWB systems in indoor environments. The analysis motivated an approach to improve the transmission range of UWB systems by using linear precoding and multiple antennas. Linear precoding allows a more efficient use of the rich spectral diversity in UWB systems, and multiple antennas exploit the spatial diversity to combat fading. Both techniques can effectively improve the transmission range of UWB devices.

7. REFERENCES

[1] L. Yang and G. B. Giannakis, "Ultra-wideband communications: An idea whose time has come," *IEEE Signal Processing Mag.*, vol. 21, pp. 26–54, Nov. 2004.

[2] "New public safety applications and broadband internet access among uses envisioned by FCC authorization of ultra-wideband technology", *revision of part 15 of the commission's rules regarding ultra-wideband transmission systems*, Federal Communications Commission (FCC), Washington, D.C. 20554, February 14, 2002.

[3] "MultiBand OFDM physical layer specification," *MultiBand OFDM Alliance Special Interest Group*, 2005.

[4] J. R. Foerster, M. Pendergrass, and A. F. Molisch, "A channel model for ultrawideband indoor communication," *IEEE 802.15.3a standardization group*, 2003.

[5] A. Batra, J. Balakrishnan, G. R. Aiello, J. R. Foerster, and A. Dabak, "Design of a multiband OFDM system for realistic UWB channel environments," *IEEE Trans. Microwave Theory Tech.*, vol. 52, pp. 2123–2138, Sep. 2004.

[6] R. D. Wesel, "Convolutional codes," in *Wiley Encyclopedia of Telecommunications*, J. G. Proakis, Ed., vol. 1, pp. 598-606, New Jersey: Wiley, 2003.

[7] Y. Xin, Z. Wang, and G. B. Giannakis, "Space-time diversity systems based on linear constellation precoding," *IEEE Trans. Wireless Commun.*, vol. 2, pp. 294–309, Mar. 2003.

[8] A. H. Sayed, *Fundamentals of Adaptive Filtering*. New Jersey: Wiley, 2003.